ISSN 1392 - 1207. MECHANIKA. 2012 Volume 18(1): 35-39

Dynamic monitoring the strain of composites due to high speed collisions using fiber bragg grating network

Zeyu Hu*, Yifan Hu**
**Department of Control Science and Engineering, Huazhong University of Sci. and Tech., Wuhan, 430074, China; E-mail: 642902854@qq.com*
***Department of Physics, Huazhong University of Sci. and Tech., Wuhan, 430074, China; E-mail: yifanhu2007@yahoo.com*

crossref http://dx.doi.org/10.5755/j01.mech.18.1.1277

1. Introduction

High speed collision can result in serious consequences; for example, high speed train, airplane, aircraft etc. which are in the movement with high speed might encounter this kind of problem. On the other hand, the application of advanced composites to large commercial aircrafts has recently increased in light of the demand of reduced operation cost from airlines, emphasis on energy saving, lower-cost materials, [1]. The damages occurring in composite materials are caused by several types of impacts, such as bird strikes, hail, dropping of tools, etc. The damages of composite caused by high speed collision can probably be detected by measuring the dynamic strain at appropriate locations of the structure [2]. We have been designing a damage monitoring system that can detect the changes of strain and deformation of composite materials using an Fiber Bragg Grating (FBG) optical fiber system [3]. It was verified that this system was superior as compared to the conventional nondestructive inspection (NDI) system.

2. The basic mechanism of FBG mechanics sensor

The grating was formed at the core of GeO2-doped optical fiber by exposing it to UV laser and making repetitive layers whose refractive index of the core changes continuously with the distribution of the interference pattern of the laser [4]. When beam goes through FBG, multiple Fresnel Reflection will take place in the whole grating area. If the wavelength doubles the length of grating, reflected beam and incidence beam meet together, and form constructive interference, i.e. it will result in a narrow band reflective wave (Fig. 1) [5]. The wavelength of the reflective wave is called Bragg wavelength λ_B

$$2n_{eff}\Lambda=\lambda_B \tag{1}$$

where n_{eff} is effective refractive index and Λ is period of the grating.

From (1), one can see that a perfect optical fiber sensor can be made by FBG. If wavelength does not satisfy the condition of Bragg interference, it will pass FBG with low loss. When the physical parameters, such as temperature, electromagnetic field, are changing, the stress on the optical fiber grating will change too, and it will lead to the change of Bragg wavelength.

The FBG sensors in the fiber reflect a specific wavelength of the light signal back to the Demultiplexing Interrogation system, from which the value of strain can be determined.

One can see that more clearly by differentiating the equation (1)

$$\Delta\lambda_B=2n_{eff}\Delta\Lambda+2\Delta n_{eff}\Lambda \tag{2}$$

where $\Delta\Lambda$ is the elastic deformation of optical fiber under strain and Δn expresses the elastic-optical effect of optical fiber under strain.

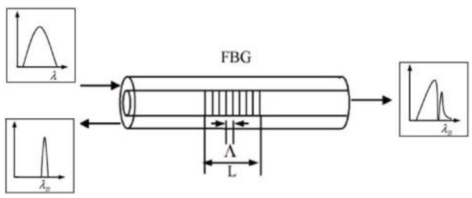

Fig. 1 A broadband light spectrum is transmitted through a glass fiber by a super luminescent LED (SLED)

$\Delta\lambda_B$ can be measured by the system showed in Fig. 1. When FBG is compressed, then Bragg wavelength will be blue shifted. While tensile the FBG, then Bragg wavelength will be red shifted. From (2), one can get the quantitative relation between Bragg wavelength increment and strain increment if the modulus of the optical fiber and elastic-optic constant are known. When optical grating is affected only by the axial elasticity, one can get the relation between Bragg wavelength increment and external force and the parameters of the optical fiber material from formula (1) and (2).

$$\frac{\Delta\lambda_B}{\lambda_B}=\frac{\Delta\Lambda}{\Lambda}+\frac{\Delta n_{eff}}{n_{eff}} \tag{3}$$

From reference [6], the relative change of wavelength can be expressed as

$$\left(\frac{\Delta\lambda_B}{\lambda_B}\right)_z=-\frac{n_{eff}^2}{2}\left(p_{11}\varepsilon_{rr}+p_{12}\varepsilon_{rr}+p_{12}\varepsilon_{zz}\right)+\varepsilon_{zz} \tag{4}$$

where p_{11} and p_{12} are two components of elastic-optic constant of the optical grating.

ε_{zz} is the strain alone the Z-axis, while ε_{rr} is the strain alone the radial direction. When the change of temperature is negligible, the variance of refractive index and grating period come mainly from the variance of the stress.

Considering the simplest situation with merely uniform axial stress: $\sigma_{zz} = -P$ and $\sigma_{rr} = \sigma_{\theta\theta} = 0$ (where σ_{zz} is the stress alone the Z-axis, (σ_{rr} is the stress alone the radial direction; $\sigma_{\theta\theta}$ is the stress alone the section from $\vec{e}_\theta$ direction; P is external pressure). According to generalized Hook′s law, strains from all directions are [7]

$$\begin{bmatrix} \varepsilon_{rr} \\ \varepsilon_{\theta\theta} \\ \varepsilon_{zz} \end{bmatrix} = \begin{bmatrix} \eta \dfrac{P}{E} \\ \eta \dfrac{P}{E} \\ -\dfrac{P}{E} \end{bmatrix}. \tag{5}$$

3. The basic optical and electronic devices

FBG network is a number of different types of FBG in one or several optical fiber FBG array constituted by series-parallel. It will facilitate the achievement of real-time measurements with multicomponents, and sense 5 parameters of signal characteristics (wavelength, phase, polarization, propagation direction and amplitude). To conduct multipoint measurement, it is necessary to use address multiplexing. Sensor array codes address with different Bragg reflection wavelength. Bragg reflection wavelength bandwidth is about 0.3 nm bandwidth. To each sensor is assigned a unique wavelength range. By using the input broadband signal of a same broadband light source to each FBG, the grating reflection peak in each respective change within the wavelength range.

There are several methods for demodulation of all reflected waves. But only the interference method and mode-locked modulation are suitable for the dynamic situations. Demodulation solutions based on interference, according to the type of interferometer, can be divided into Mach-Special (M-Z) unbalanced fiber interferometer demodulation and nonequilibrium scan Michelson interferometer demodulation. The nonequilibrium M-Z interferometer was developed by Kersey A.D [8]. Compared with other demodulations, M-Z interferometer is simpler and more accuracy. The schematic diagram is shown in the Fig. 2. It is a two 3dB coupler series connection, and the lengths of the interferometer arms are not equal, with a difference of *d*. As shown in Fig. 2, *2* is the input arm, and the input is the narrowband light with $\Delta\lambda$ bandwidth of fiber grating. *3* and *4* are the interferometer output arms. Bragg wavelength is the wavelength of reflected light in the case of fiber Bragg grating without added stress.

According to the coupling theory, when the two output arms of the optical path are different, there is an optical path difference nd (n is the refractive index of fiber), the phase difference corresponding is

$$\phi = \frac{2\pi dn}{\lambda} \tag{6}$$

When d and n do not change with the environment, due to the change in strain reflection wavelength changes

$$\Delta\lambda_B = \lambda_B k\varepsilon \tag{7}$$

Phase difference of the interferometer output caused by wavelength shifting is

$$\Delta\phi = \frac{2\pi dn}{\lambda_B^2}\Delta\lambda_B = \frac{2\pi dn}{\lambda_B}k\varepsilon \tag{8}$$

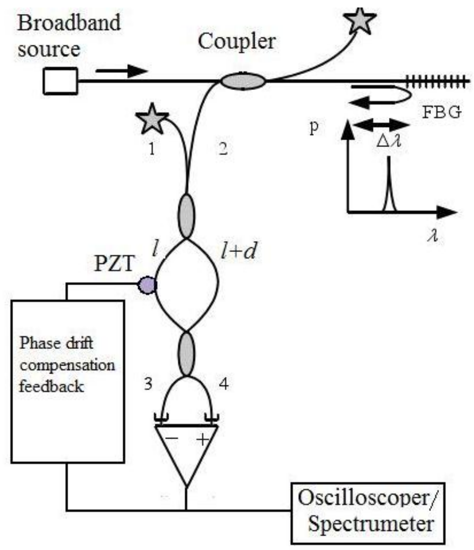

Fig. 2 The block diagram of whole optical and electronic elements

It can be seen from the above equation that, as long as the amount of phase change $\Delta\phi(\Delta\lambda)$ can be detected, one can know the change of wavelength and the amplitude of stress wave. This detection method is easily implemented on signal detection. However, a key issue is how to calibrate coefficient *k*. General approach is to use piezoelectric (PZT) ceramics to make a steady change in the optical path difference. Since the relationship between withstand strain to the piezoelectric ceramic and the voltage is linear, so by knowing the increase of the voltage and phase variation to the piezoelectric ceramics, one can calibrate *k*. But the light energy back from the PZT will have a great attenuation which is a big trouble for the test. In addition, when the fiber has not only the longitudinal strain, but also transverse strain as well, it would have secondary effects, photo elastic effect, in which $\Delta\lambda$ is given by Eq. (3). Those environmental factors cause relationships between horizontal and vertical strain and phase difference can be expressed as

$$\Delta\phi = \frac{2\pi nd}{\lambda_B}\left\{\left[\frac{\Delta\lambda a}{\lambda\Delta a} - \frac{n^2}{2}\left(P_{11}+P_{12}\right)\right]\varepsilon_{rr} + \left(1-\frac{n^2}{2}P_{12}\right)\varepsilon_{zz}\right\}. \tag{9}$$

4. The three-dimensional stress measurements

In order to get the direction and intensity of the stress wave, accurate multicomponent measurement is necessary. Multicomponent force measurement includes the measurements of the vertical stress and the paralleling stress (shear stress) to the surface. Only by an objective and complete measurement of the pressure and shear stresses, can we get the information of the three-dimensional stress distribution in different parts of the material after the collision.

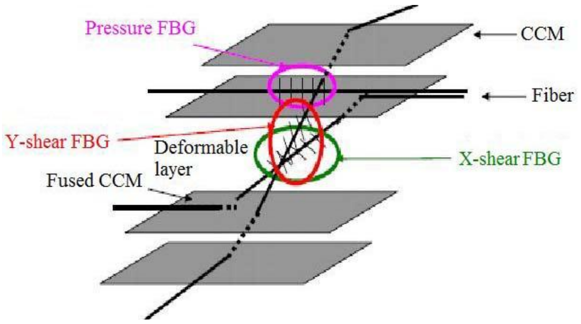

Fig. 3 The schematic design of the multicomponent measurement system

Since the relationship among the change of Bragg wavelength, the axial strain, Poisson ratio and elastic modulus is more straightforward, measuring axial strain is relatively easy [6]. Therefore, in order to achieve accurate measurement, it is necessary to set the network with three-dimensional distribution of fiber Bragg grating, trying best to use axial mechanical parameters in three directions which measured from the changes of reflected Bragg wavelength. The schematic design of this system is shown in Fig. 3. First, for the pressure measurement, the FBG is embedded within the layers of a carbon composite material (CCM). Under the pressure, FBG sensor will be under compression or tension corresponding to embedded upper layer or lower layer, respectively. Thus, the pressure can be transferred as axial strain through compression or tension [9]. For shear force measurement, the FBG is embedded at a very small angle (1-5°) with in the CCM layer. A deformable layer (Silicon rubber) is introduced between the upper and lower layers of CCM. With this embedding technique, a relative motion between the upper and lower layers will take place when the shear force is applied to the upper layer of the CCM. This relative motion between the upper and lower layers will stretch or compress the embedded fiber, which will result in a change of the fiber length and thus changing the reflected Bragg wavelength. Based on this principle, a 3D force sensor system can be fabricated.

5. The precise positioning technologies

The measured data from the three-dimensional network of multichannel FBG obtained by embedding multicomponent measurements of stress can tell us the distribution of wave magnitude and direction of the stress. Based on the further analysis of retrieval data from stress distribution, the wave sources, i.e. the location of the collision took place, and collision strength could be deduced. In order to locate the collision position, Time Difference Positioning (TDP) technology will be used. TDP can be divided into one-dimensional plane location, two-dimensional and three-dimensional spherical or cylinder positioning. TDP technology is based on the measurement of the time difference in which shock wave arrives every FBG probe distributed in different position, wave propagation velocity, and processing these measured data to determine the coordinates of the wave source as shown in Fig. 4 [10].

Plane or cylinder positioning can be achieved by three sensors. Assuming that the stress wave propagation velocity in all directions is constant V (media surface velocity), and the sensor 1 is the closest probe from the collision point, one can easily get the shock wave arrival order, arrival time, the time difference of sensor 2 and 3, as well as following series of equations [10]

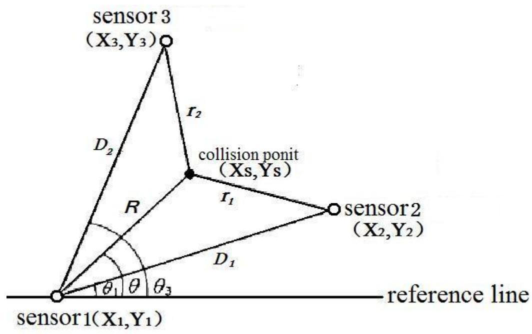

Fig. 4 Infinite plane collision point positioning of three probes

$$\Delta t_1 V = r_1 - R \tag{10}$$

$$\Delta t_2 V = r_2 - R \tag{11}$$

$$R = \frac{1}{2}\frac{D_1^2 - \Delta t_1^2 V^2}{\Delta t_1 V + D_1 \cos(\theta - \theta_1)} \tag{12}$$

$$R = \frac{1}{2}\frac{D_2^2 - \Delta t_2^2 V^2}{\Delta t_2 V + D_2 \cos(\theta_3 - \theta)} \tag{13}$$

From the equations, positioning can be easily realized.

6. Precise determination of the damage region

During whole propagation process, the strain wave propagation property might be different in plastic deformation region and elastic region. Thus, through studying the propagation property of the strain wave front, one can determine the plastic deformation region. Consider the original length along the fiber axis is a unit of dx. A non-balance force in the x direction is

$$dF = A\frac{\partial \sigma_{zz}}{\partial x}dx \tag{14}$$

The force acts on the unit with mass of $\rho A dx$, where ρ and A are mass density and cross-sectional area respectively, by Eq. (4)

$$\sigma_{zz} = E\varepsilon \tag{15}$$

Strain ε is related to the displacement u along the x direction $\varepsilon = \partial u / \partial x$, $v = \partial u / \partial t$; v is the propagation speed. The motion equation of stress is

$$\rho\frac{\partial^2 u}{\partial t^2} = \frac{d\sigma}{d\varepsilon}\frac{\partial \varepsilon}{\partial x} \tag{16}$$

Considering an optical fiber as a semiinfinite rod, a stretch (or compression) is imposed on the rod. Let the $t = 0$, $x = 0$ and with a velocity v_0, and the boundary conditions are: $x = 0$, $v = v_0$; or $x = -\infty$, $v = 0$ to solve the equation (16), let $\xi = x/t$ because the elastic modulus is a function of strain

$$E = E(\varepsilon), \quad \varepsilon = f(\xi) \tag{17}$$

so

$$u = \int_{-\infty}^{x} \frac{\partial u}{\partial x} dx = \int_{-\infty}^{x} f(\xi) dx = t \int_{-\infty}^{x} f(\xi) d\xi \tag{18}$$

let

$$\xi = x/t, \quad \frac{\partial^2 u}{\partial t^2} = f'(\xi) \frac{\xi^2}{t} \tag{19}$$

one can get

$$f'(\xi)\left(\rho \xi^2 - E\right) = 0 \tag{20}$$

so

$$f'(\xi) = 0, \quad \frac{x}{t^2}^2 = \frac{E}{\rho}, \quad \varepsilon = 0 \tag{21}$$

These three solutions were effective in three different regions, according to reference [11], which can be simply defined to be the plastic region, elastic region and zero deformation region. The interface of the plastic region and the elastic region are known as the plastic wave front $\xi = c_1$. The interface of elastic region and the interface region of zero deformation is called elastic wave front $\xi = c_0$ c_1 and c_0 can be experimentally determined, as shown in Fig. 4. Then the solution of Eq. (16) can be written as

$$\text{when } |x| < c_1 t \quad \varepsilon = \text{constant} = \frac{v_1}{c_1} = \varepsilon_1 \tag{22}$$

$$\text{when } c_1 t < |x| < c_0 t \quad E(\varepsilon) = \frac{\rho x^2}{t^2} \tag{23}$$

$$\text{when } |x| > c_0 t \quad \varepsilon = 0 \tag{24}$$

Take the above results into Eq. (4), wavelength variation over time and space can be obtained.

7. Conclusions

We propose a preliminary design of damage monitoring system for real-time measurements of high speed collision including the position, intensity, damage assessment. By discussing the monitoring the strains caused by high speed collisions in composite using FBG sensors, shock wave propagation characteristics, and theoretical study on optical and electronic system, it demonstrates that this design is feasible. The following conclusions can be obtained:

1. FBG sensor network can detect the dynamic stress and strain by detecting the changes in the wavelength.

2. It can also tell the information about the source of those stress and strain, such as the collision position, intensity, damage intensity, and achieve the monitoring of the high speed collision which results in the change of a series of physical parameters.

3. Fiber Bragg Grating Network might possess some good properties such as sensitive, high speed, low cost, light weight, stable, and might be suitable for spacecraft and other high speed devices.

References

1. **Zabulionis, D.; Gailius, A.** 2007. Numerical modelling of creep functions of laminated composites, Mechanika 3(65): 5-11.
2. **Noritsugu, N. et al**. 2007. Impact monitoring of the aircraft composite structure using FBG sensor/PZT actuator hybrid sensor system, Proc. of SPIE, 6527 65270B-1. http://dx.doi.org/10.1117/12.715584
3. **Hill, K.O.; Fuji, Y., Johnson, D.C.; Kawasaki, B.S**. 1978. Photosensitivity in optical fiber waveguides: application to reflection fiber fabrication, Appl Phys Lett 32(10): 647-455. http://dx.doi.org/10.1063/1.89881
4. **Meltz, G.; Morey, W.; Glenn Hill, W.** 1989. Formation of Bragg grating in optical fiber by the transverse holographic method, Opt Lett 14(15): 823-827. http://dx.doi.org/10.1364/OL.14.000823
5. Eric Kosters and Thomas J. van Els. 2010. Structural health monitoring and impact detection for primary aircraft structures, Proc. of SPIE, 7677 76770C-1. http://dx.doi.org/10.1117/12.853013
6. **Butter, C.D.; Hucker, G.B.** 1978. Fiber optic strain gauge, Appl Opt., 17(18): 2867-2869. http://dx.doi.org/10.1364/AO.17.002867
7. **Liao, Y.B**. 2000. Fiber Optics, Beijing, Tsinghua University Press.
8. **Kersey, A.D.; Berkoff, T.A.; Morey, W.W**. 1992. High-Resolution Fiber–Grating Based Strain Sensor with Interferometer wave-Length-Shift Detection, Electronic Lett 28(3): 236-238. http://dx.doi.org/10.1049/el:19920146
9. **Suresh R., Tjin S.C., Bhalla S.** 2009. Multi-component force measurement using embedded fiber Bragg grating, Optics & Laser Technology 41: 431-440. http://dx.doi.org/10.1016/j.optlastec.2008.08.004
10. **Pascale, G.; Di Leo, A.; Carli R.; Banora, V.** 2000. Evaluation of actual compressive strength of high strength concrete by NDT, [A]. Proc of 15th WCNDT [M/ CD] Rome: 2000. 527.
11. **Duwez, P.E.; Clark D.S.; Bohnenblust, H.F.** 1950. The behavior of long beams under impact loading, J. Appl. Mech., Truns. 17(1): 27-34.

Zeyu Hu, Yofan Hu

KOMPOZITŲ DEFORMACIJŲ DINAMINĖ STEBĖSENA ESANT DIDELIO GREIČIO SUSIDŪRIMAMS NAUDOJANT PLUOŠTINIO BRAGO TINKLELIO SCHEMĄ

R e z i u m ė

Šiame straipsnyje aprašoma pluoštinio Brago tinklelio sensoriaus sistema, naudojama dinaminių deformacijų stebėsenai esant didelio greičio susidūrimams. Autoriai tiria, kaip ši sistema panaudojama realaus laiko didelio greičio susidūrimo smūgiui ir sukeltam pažeidimui nustatyti. Trijų deformacijos komponentų sensoriaus sistema buvo preliminariai suprojektuota susidūrimo padėčiai ir pažeidimo laipsnio realiam laikui nustatyti atsižvelgiant į tampriąją ir plastinę deformacijas. Straipsnyje aprašytos pagrindinės optinės ir elektroninės šios sistemos teorijos, taip pat modelio sensoriaus mechanizmas ir mechanika.

Zeyu Hu, Yofan Hu

DYNAMIC MONITORING THE STRAIN OF COMPOSITES DUE TO HIGH SPEED COLLISIONS USING FIBER BRAGG GRATING NETWORK

S u m m a r y

This paper describes the Fiber Bragg Grating (FBG) sensor system for a dynamic monitoring strain due to high speed collision. The authors investigate whether or not this FBG system can be used for the real time detection of both the impact and the damage generated by high speed collisions. A three-component strain sensor system was preliminary designed for real-time detection the location of collision and the damage extent such as the ranges of the elastic deformation and the plastic deformation. The basic optical and electronic theories about this system, as well as the mechanism and mechanics model of FBG sensors, are expressed in this paper.

Keywords: dynamic monitoring, composites, fiber bragg grating network.

Received February 17, 2011
Accepted January 11, 2012